analytical chemistry

Article

pubs.acs.org/ac

High-Sensitivity Measurement of Density by Magnetic Levitation

Alex Nemiroski,*[,†] A. A. Kumar,[†] Siowling Soh,[†] Daniel V. Harburg,[†] Hai-Dong Yu,[†] and George M. Whitesides*[,†,‡,§]

[†]Department of Chemistry and Chemical Biology, [‡]Wyss Institute for Biologically Inspired Engineering, and [§]Kavli Institute for Bionano Science and Technology, Harvard University, Cambridge, Massachusetts 02138, United States

Supporting Information

ABSTRACT: This paper presents methods that use Magnetic Levitation (MagLev) to measure very small differences in density of solid diamagnetic objects suspended in a paramagnetic medium. Previous work in this field has shown that, while it is a convenient method, standard MagLev (i.e., where the direction of magnetization and gravitational force are parallel) cannot resolve differences in density $<10^{-4}$ g/cm^3 for macroscopic objects (>mm) because (i) objects close in density prevent each other from reaching an equilibrium height due to hard contact and excluded volume, and (ii) using weaker magnets or reducing the magnetic susceptibility of the medium destabilizes the magnetic trap. The present work investigates the use of weak magnetic gradients parallel to the faces of the magnets as a means of increasing the sensitivity of MagLev without destabilization. Configuring the MagLev device in a rotated state (i.e., where the direction of magnetization and gravitational force are perpendicular) relative to the standard configuration enables simple measurements along the axes with the highest sensitivity to changes in density. Manipulating the distance of separation between the magnets or the lengths of the magnets (along the axis of measurement) enables the sensitivity to be tuned. These modifications enable an improvement in the resolution up to 100-fold over the standard configuration, and measurements with resolution down to 10^{-6} g/cm^3. Three examples of characterizing the small differences in density among samples of materials having ostensibly indistinguishable densities—Nylon spheres, PMMA spheres, and drug spheres—demonstrate the applicability of rotated Maglev to measuring the density of small (0.1−1 mm) objects with high sensitivity. This capability will be useful in materials science, separations, and quality control of manufactured objects.

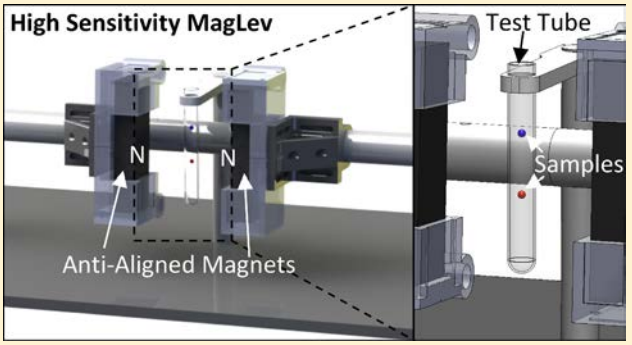

This Article describes ways to increase the sensitivity of magnetic levitation (MagLev)—a method that maps the density of a diamagnetic object on to its position suspended in a paramagnetic medium—to small differences in density without increasing the complexity of system. The ability to resolve very small differences or changes in density—a universal, physical property of matter[1,2]—is important for many applications, such as (i) the quality control of manufactured products (e.g., of food,[3] alcoholic contents in liqueur,[4] and biofuel[5]), (ii) the diagnosis of diseases (e.g., by examining biological samples such as urine[6] and blood,[7−9] and (iii) the evaluation of thermophysical properties (e.g., isothermal compressibility coefficient and thermal expansion coefficient) useful for characterizing and optimizing industrial manufacturing processes involving various substances (e.g., solids,[10] liquids,[11,12] mixtures of liquids,[13] amino acids,[14] polypeptides,[15] drugs,[16] and many others[17−19]). Density is also a parameter used to determine other important properties of materials (e.g., elastic modulus,[20,21] compressibility of proteins,[22] stability of pharmaceutical products,[23] and glass-forming ability[24]) or other types of behaviors (e.g., kinetics of crystallization[25] and metastable states[26]).

A variety of systems or devices are available for measuring density, including hydrometers, density-gradient columns, pycnometers, oscillating-tube densitometers, suspended microchannel resonators,[27] and magnetic suspension balances.[28] These methods, however, are often nonportable, difficult to use, or expensive.[1,27] A number of them can only measure the density of fluids; measurements of densities of small (<1 mm) soft, heterogeneous, and irregularly shaped solids, waxes, and gels are especially difficult. MagLev is a versatile method to measure directly the density of solid or liquid diamagnetic samples (of arbitrary shape). This method has three characteristics that are advantages in particular circumstances: (i) it is inexpensive (the NdFeB magnets cost ∼$5−50 each), (ii) it operates without electricity, and (iii) it is portable.

Briefly, MagLev uses two magnets that are antialigned, and a paramagnetic liquid to create a magnetic energy well at the midpoint between the faces of the magnets.[29] A diamagnetic object will be pushed into this well, while gravity acts to counteract this force, and to displace the object away from the

Received: October 16, 2015
Accepted: January 27, 2016
Published: January 27, 2016

DOI: 10.1021/acs.analchem.5b03918
Anal. Chem. 2016, 88, 2666−2674

center; the object sinks down if it is denser than the medium, and rises up if it is less dense. The density can be determined by measuring the position of the objects—its "levitation height"—relative to the faces of the magnets. MagLev, therefore, is a simple system that enables differences in the densities between an object and the medium, or between different objects, to be calculated using measurements of levitation height. We have previously shown that this simple method can be used to distinguish atomic-level differences in chemical composition,[30] monitor chemical reactions,[30] measure binding constants of protein−ligand interaction,[31] determine nutritionally relevant properties of food and salinity of water,[32] analyze forensic evidence,[33] orient nonspherical objects in three-dimensions,[34] and perform nondestructive quality control on plastic components.[35] We and others have also used MagLev for 3D self-assembly,[36−38] and others have used MagLev to separate mammalian cells with different densities,[39] and coupled MagLev with smartphones for automated analysis of density.[40]

Although we have previously demonstrated a measurement resolution of 2×10^{-4} g/cm^3 for narrow ranges of densities,[29] many applications—such as evaluating cerebrospinal fluid and high purity fuels,[16,41−43] or detecting small changes in density (e.g., binding of proteins on a surface)—require even higher resolution in density to measure small changes in composition or impurities. Further increase of the sensitivity without geometric modifications of the system runs into two major challenges: (i) objects close in density prevent each other from reaching equilibrium height due to excluded volume, and (ii) objects close in density cannot be resolved by eye without magnification.

Here, we investigate ways to increase the resolution in density of MagLev by enhancing the sensitivity (distance between objects levitating at equilibrium per unit density) to differences in density through various modifications of the magnetic configuration that do not compromise the stability or simplicity of the method. In general, sensitivity and range are coupled in MagLev. We have recently shown that "tilting" the MagLev device, relative to the gravitational vector, can yield up to a 15× increase in the range of densities that can be measured simultaneously, at the expense of sensitivity.[44] In this Article, we explore the relative weakness of the horizontal restoring force as a means to decrease the magnetic field gradient and increase the sensitivity, at the expense of range, along the axis of measurement. Specifically, we show that the sensitivity of MagLev can be tuned in two simple ways. (i) By rotating the entire MagLev device relative to gravity, we show that it is possible to continuously tune the separation distance between levitating objects. (ii) By altering the aspect ratio of the MagLev configuration (by changing the length, width, or height of the magnets, or the distance between them), we show that it is possible to tune the gradients of the magnetic field and hence the sensitivity along the different axes. We call this approach "rotated MagLev" to emphasize the specific utility of the apparatus when it is rotated fully perpendicular to the gravitational vector to enable simple, high-sensitivity measurement of density. We contrast this description with our previous investigation of "tilted MagLev", which emphasized gradual tuning of linear range by tilting the apparatus (with container), but not rotating it fully perpendicular to the gravitational vector.

Through a combination of these procedures, we show that the sensitivity of MagLev to differences in density can be increased, in a practical manner, up to 100× over previous measurements. We discuss the physical principle for the increase of sensitivity (increased separation between the objects) when MagLev is rotated, and the levitation path of diamagnetic objects for intermediate angles, by examining the balance of forces involved in maintaining the objects at their equilibrium positions. We measure differences in density with a resolution down to 2×10^{-6} g/cm^3 and demonstrate the usefulness of tuning the sensitivity in these ways in two important applications by examining the quality of calibration standards and the density distribution in density of drug spheres.

EXPERIMENTAL SECTION

We purchased two sets of NdFeB magnets for experiments: (i) 2 × 1 aspect ratio ($L \times W$ = 4 in. × 2 in.; H = 1 in.; strength N40) and (ii) 3 × 1 aspect ratio ($L \times W$ = 6 in. × 2 in.; H = 1 in.; strength N42) from www.k&jmagnetics.com. To mount the magnets, we fabricated two sets of housings by 3D-printing (Fortus 250mc, Stratasys) ABS plastic. To control the angle of rotation, we fixed the magnet housings to a rotating mechanism constructed from standard optical mounting components purchased from Thorlabs. We purchased all density standards from American Density Materials, Inc., Nylon and PMMA spheres from McMaster-Carr, and Prevacid drug capsules from Novartis Consumer Health, Inc. We used data and procedures reported by Mirica et al.[29] and Bwambok et al.[45] to determine the densities and magnetic susceptibilities of solutions with different concentrations of $MnCl_2$, $GdCl_3$, and $ZnCl_2$. We include further information about the experimental design, including safety considerations, in the Supporting Information (SI).

RESULTS AND DISCUSSION

Tilted Magnetic Levitation. In this section, we investigate the behavior of diamagnetic objects in a MagLev device undergoing rotation relative to the direction of gravity. Figure 1a defines the standard MagLev configuration: a diamagnetic sample—with volume $\boldsymbol{V}$ (m^3), density ρ_s (kg/m^3), and magnetic susceptibility χ_s (unitless)—is introduced into a paramagnetic solution (e.g., aqueous $MnCl_2$)—with density ρ_m and magnetic susceptibility χ_m—that is contained in a transparent, nonmagnetic container that is placed between two, flat permanent magnets arranged with like poles facing each other. We place the origin of the coordinate system at the midpoint between the faces of the magnets and define the MagLev frame of reference by coordinates x, y, z and the laboratory frame of reference by the coordinates x', y', z'; the coordinate systems are related by a rotation matrix and the magnetic field is $\mathbf{B}(x, y, z)$. The difference in magnetic susceptibility between the sample and medium is $\Delta\chi \equiv \chi_s - \chi_m$ and the difference in densities is $\Delta\rho \equiv \rho_s - \rho_m$.

The magnetic force on a spherical object with homogeneous density and susceptibility is, in general, given by $\mathbf{F}_{mag} = \frac{\Delta\chi V}{2\mu_0}(\mathbf{B}\cdot\nabla)\mathbf{B}$ and the force of gravity acting on the object is constant and given by $\mathbf{F}_{grav} = -\Delta\rho V g\hat{\boldsymbol{z}}'$. In these equations, g is the acceleration due to gravity (9.810 m/s^2), μ_0 is the magnetic permeability of free space ($4\pi \times 10^{-7}$ N/A^2), B is expressed in SI units (T = kg A^{-1} s^{-2}), vectors are represented by the characters in bold, and ∇ represents gradient in three dimensions. An object levitates stably when $\mathbf{F}_{mag} + \mathbf{F}_{grav} = 0$; the equilibrium positions can be found, in general, by solving eq 1 for a chosen magnetic configuration.

DOI: 10.1021/acs.analchem.5b03918
Anal. Chem. 2016, 88, 2666−2674

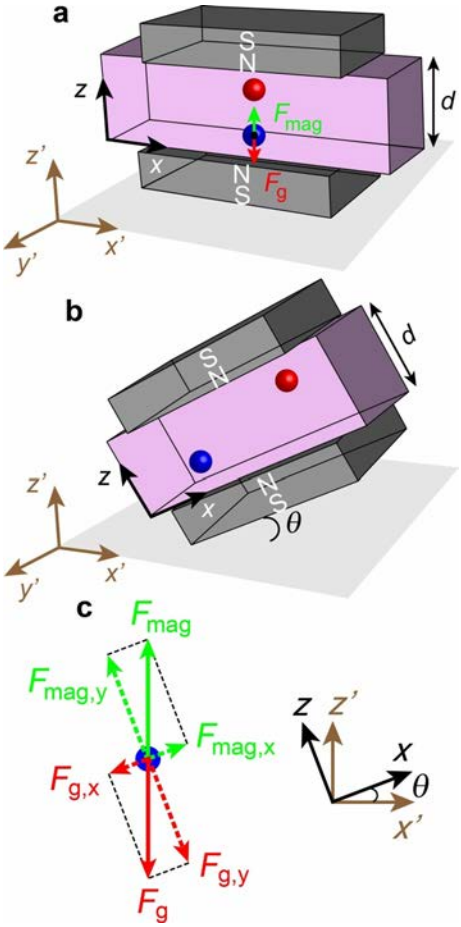

Figure 1. Illustration of the Magnetic Levitation (MagLev) device and the forces involved in levitating objects. (a) MagLev consists of a paramagnetic solution placed between two magnets with like poles facing each other. Diamagnetic objects levitate in equilibrium due to the balance of gravitational force, F_g, and the magnetic force, F_{mag}. (b) To increase the sensitivity of density measurement, the MagLev device is rotated by an angle, θ, about the y' axis (absolute frame of reference). The x and z axes are defined to rotate together with the device. (c) When the MagLev device is rotated, the forces involved (F_g and F_{mag}) can be resolved into two components with respect to the x and z axes.

These and related equations are also described in detail elsewhere.[26]

$$\frac{\Delta\chi}{2\mu_0}(\mathbf{B}\cdot\nabla)\mathbf{B} = \Delta\rho g\hat{z}' \tag{1}$$

If we rotate the entire MagLev device by an angle θ about the y'-axis (Figure 1b), relative to the laboratory frame of reference, then $\hat{z}' = (\sin\theta, 0, \cos\theta)$ and eq 1 yields eqs 2 and 3.

$$\frac{\Delta\chi}{2\mu_0}(\mathbf{B}\cdot\nabla)B_z = \Delta\rho g\cos\theta \tag{2}$$

$$\frac{\Delta\chi}{2\mu_0}(\mathbf{B}\cdot\nabla)B_x = \Delta\rho g\sin\theta \tag{3}$$

For a chosen pair of magnets with length L along the x-axis, width W along the y-axis, height H along the z-axis, distance d between antialigned faces, and remnant magnetization B_r (provided by the manufacturer), the magnetic field $\mathbf{B}(x, y, z)$ can be easily found by calculation using finite element analysis (e.g., with COMSOL Multiphysics).

To investigate this behavior, we configured a typical geometry for performing MagLev (NdFeB magnets, $L \times W \times H$ = 4 in. × 2 in. × 1 in., d = 5 cm, B_s = 0.3 T). We refer to this configuration as the $L \times W$ = 2 × 1 aspect ratio. Figure 2

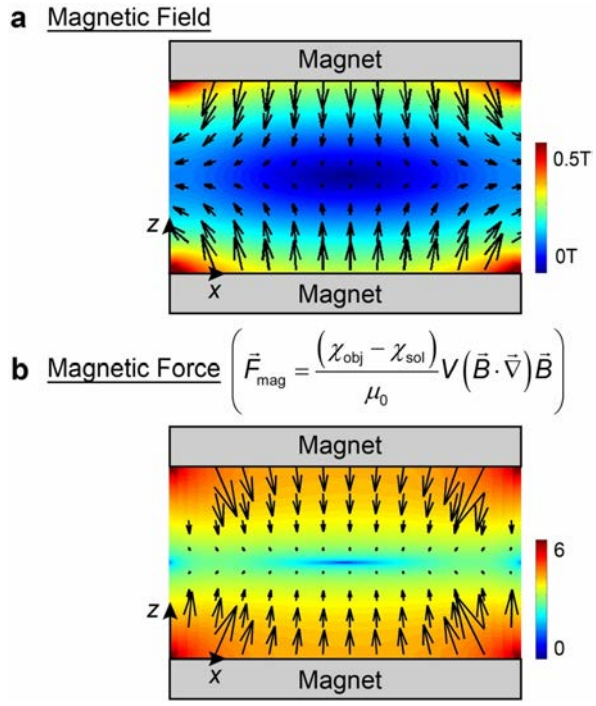

Figure 2. (a) A slice of the simulated three-dimensional magnetic field in the x–z plane at the middle of the device with respect to the y-axis. (b) Plot of the F_{mag}. The surface plot shows the logarithm of the magnitude of the magnetic force $\log|F_{mag}|$. Arrows indicate the direction and magnitude of the force.

shows a plot of the expected magnitude and direction of $\mathbf{B}(x, y, z)$ and $\mathbf{F}_{mag}(x, y, z)$ calculated with COMSOL. We demonstrated this principle by levitating five beads (American Density Materials, Inc.) of known densities—1.0810 g/cm^3 (red), 1.0900 g/cm^3 (colorless), 1.1000 g/cm^3 (blue), 1.1100 g/cm^3 (colorless), and 1.1200 g/cm^3 (yellow)—in an acrylic container filled with an aqueous paramagnetic solution (1.00 M $MnCl_2$). We rotated the device successively in intervals of 1° (from 0° to 35°), and captured an image of the device at each interval. We quantified the angle of rotation and the displacement of each bead from the center of the device in both x and z directions with Adobe Photoshop CS4. Figure 3a shows the equilibrium positions of the beads changing depending on the angle of θ.

By solving eqs 2 and 3 numerically at constant θ, we obtain a family of curves that represent the equilibrium position of an object as a function of $\Delta\rho$ (isoangular lines). By solving eqs 2 and 3 numerically at constant $\Delta\rho$, we obtain a family of curves that represent the equilibrium positions for objects as a function of θ (isodensity lines). The intersection of these curves yields the equilibrium position of an object of known $\Delta\rho$ and a known rotation angle θ. Figure 3b shows a plot of the experimentally determined positions of the beads as a function of the angle of tilt superimposed with these two families of curves. The calculated results agree well with the experimental

DOI: 10.1021/acs.analchem.5b03918
Anal. Chem. 2016, 88, 2666−2674

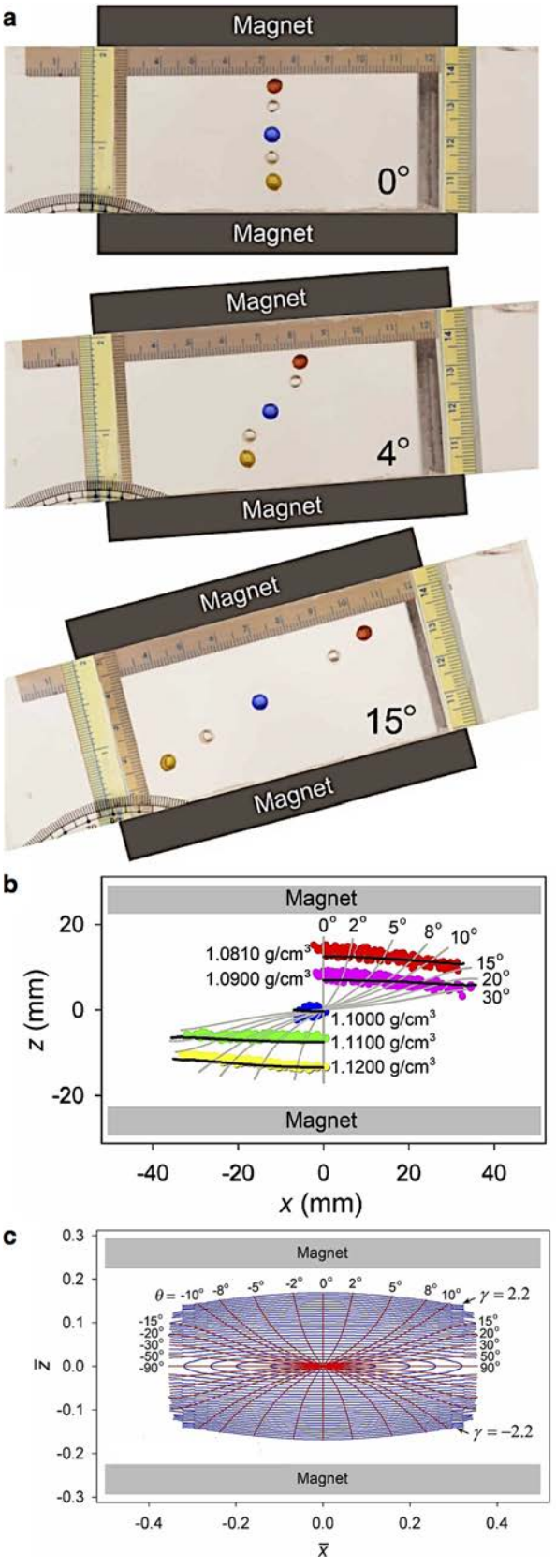

Figure 3. (a) Image showing how tilting MagLev increases the separation between the levitating objects. (b) Comparison of the simulated data with experimental data (we repeated this procedure $N = 7$ times) obtained from tilting MagLev for the five beads shown in (a). The spatial positions of the beads (with densities as indicated) are plotted for different angles of tilt for both the simulated (black lines) and experimental data (circles). The gray lines represent the positions of the beads of different densities at the specific angle as indicated. (c) Chart correlating the position of a levitating object in MagLev with the angle of tilt, θ, and a dimensionless number, γ. The blue lines represent the lines of constant γ, while the red lines represent the lines of constant angle. Once the position and θ of an object are measured, γ can be determined from the chart. The density of an object can then be calculated from γ using the formula indicated at the bottom left of the plot. Each blue line is separated by $\Delta\gamma = 0.08$.

data. Figure 3c generalizes this result by plotting isodensity and isoangular lines, for this MagLev configuration, as a function of the dimensionless parameter $\gamma \equiv (\Delta\rho g\mu_0 L)/(\Delta\chi B_s^2)$. We include further details about these calculations and measurements in the Supporting Information.

These results show that when the MagLev device is rotated, the beads spread apart because the magnetic restoring force is weaker along the x-axis than along the z-axis. This behavior suggests that the sensitivity of MagLev to differences in density can be tuned by rotation relative to the direction of gravity.

Simplifying Measurement by Rotating the Device to 90°. Because the distribution of objects for angles $0 < \theta < 90°$ follows an S-like curve, it may be difficult, in practice, to determine the density of unknown objects through simple measurements at these intermediate angles of rotation. Fortunately, at $\theta = 0°$ and $\theta = 90°$, the objects align neatly along the principle axes, thereby simplifying the determination of unknown densities. Another important benefit of the antialigned configuration is that, for many geometries, $(\mathbf{B}\cdot\nabla)\mathbf{B}$ is linear along some or all of the x-, y-, and/or z-axes. In our previous studies, where we have investigated only the configuration where the faces of the magnets remained parallel to the ground (that is, gravity acted along the z/z'-axis), and the magnets were close enough that the magnetic field along the z-axis varied approximately linearly $B(z) = B'_z z$. Empirically, we have found that this regime occurs, approximately, when $d \leq \min(L,W)$.

In the linear regime, eq 1 can be used to determine the density, $\Delta\rho$, of a diamagnetic object as a function of its measured height, Δz, as shown in eq 4.

$$\Delta\rho = \left(\frac{\Delta\chi B_z'^2}{\mu_0 g}\right) z = \frac{1}{S_z}\Delta z \tag{4}$$

Here, $S_z \equiv \mu_0 g\,(\Delta\chi B_z'^2)^{-1}$ mm/(g/cm^3) is the sensitivity of the device to differences in density (i.e., the measured distance between two objects, or between an object and the origin, per unit difference in density) and B'_z is the gradient of the field along the z-axis $(x, y = 0)$. We define the units of sensitivity to be mm/(g/cm^3), interpreted as change in levitation height (mm) per unit density (g/cm^3).

If we measured the positions of the object(s) with a measuring instrument that has a spatial resolution bounded by δ, then the resolution in density of the system $\Delta\rho_{\min}$ (the smallest quantifiable difference in density) is given by eq 3.

$$\Delta\rho_{\min} = \frac{1}{S_z}\delta_z \tag{5}$$

In defining resolution, we assume that $\delta = 1$ mm in this paper for compatibility with visual measurement using a standard ruler. For magnetic configurations with field profiles that are

DOI: 10.1021/acs.analchem.5b03918
Anal. Chem. 2016, 88, 2666−2674

nonlinear along the axis of measurement, eqs 4 and 5 only apply locally, and not throughout the entire measurement region; in these cases, these quantities remain instructive, but must be altered appropriately to incorporate the nonlinearity.

In MagLev, the sensitivity and the range of a measurement are coupled. This coupling leads to an inherent trade-off. At low sensitivity, we can interrogate a broad range of densities, but we lose our ability to resolve small differences. At high sensitivity, we can resolve small differences in density, but we are limited to densities in a narrow range close to the density of the medium. One way to expand the range of MagLev is to use a phase-separated paramagnetic solution where each phase has a different range in density.[46] The range in each liquid phase, however, still faces the fundamental trade-off between sensitivity and range. We have also previously increased the sensitivity of MagLev by decreasing the concentration of the paramagnetic salt dissolved in the medium to decrease χ_m.[29] This procedure, however, eventually encounters a fundamental limit of the system: continuing to reduce χ_m diminishes the magnetic restoring force along all axes, eventually enabling thermal fluctuations and Brownian motion to overcome the magnetic trap, randomly disperse the objects, and eliminate the correlation between height and density.

In this Article, we investigate the enhancement of sensitivity by tuning the magnetic gradient. Inspection of eq 4 shows that decreasing the magnetic gradient $B_z'^2$ increases the sensitivity and therefore improves resolution. For many configurations, the gradients along the x- and y-axes can also be linear near the center of the device and can be expressed in the same form. Therefore, when increased sensitivity (and improved resolution) is required, it is possible to rotate the MagLev device and measure along the weak gradients along x- or y-axes, relative to the standard configuration. When necessary, the sensitivity of MagLev can be further tuned by changing the aspect ratio of the magnetic configuration (moving the magnets apart or using longer magnets) to further reduce the magnetic gradient along the axis of measurement (more details in the SI).

Applications of Rotated MagLev. Here, we demonstrate the application of rotated MagLev to the quality control of (i) Nylon spheres, (ii) poly(methyl methacrylate) (PMMA) spheres, and (iii) drug spheres. In each example we show that rotated MagLev can measure distributions of density with sufficient sensitivity to characterize the variation in densities among examples of the same material that are otherwise indistinguishable.

To characterize Nylon spheres, we used the 2 × 1 MagLev configuration described in the previous section. Figure 4a shows a comparison between the sensitivities along the z- and x-axes. We then levitated five Nylon beads ($^5/_{32}$ in. diameter), in a solution of 1.70 M $MnCl_2$ with a density[29] of 1.1681 g/cm^3. At θ = 0°, this configuration had a sensitivity of S_z = 350 mm/(g/cm^3) within the linear region ±2 cm, a resolution of $\Delta\rho_{min}$ = 0.003 g/cm^3, and accommodated a range of densities of $\Delta\rho$ = 0.133 g/cm^3. Figure 4b shows how, as expected, the beads clustered at the center of the device in this standard configuration. Because of a lack of sufficient sensitivity along the z-axis to overcome exclusion of volume between the beads, in this configuration, we could not observe variations in density. Importantly, when agitated, the five beads displayed multiple, changing configurations that further hindered any consistent measurement of position, and hence density, between the beads. By contrast, Figure 4c shows that when we rotated MagLev to measure along the x-axis, the beads separated to positions that were invariant in changes to their initial state. By rotating the device to θ = 90°, we increased the sensitivity by a factor of Sz / S_x ~ 25 (S_x = 8.7 × 10^3 mm/(g/cm^3)) and

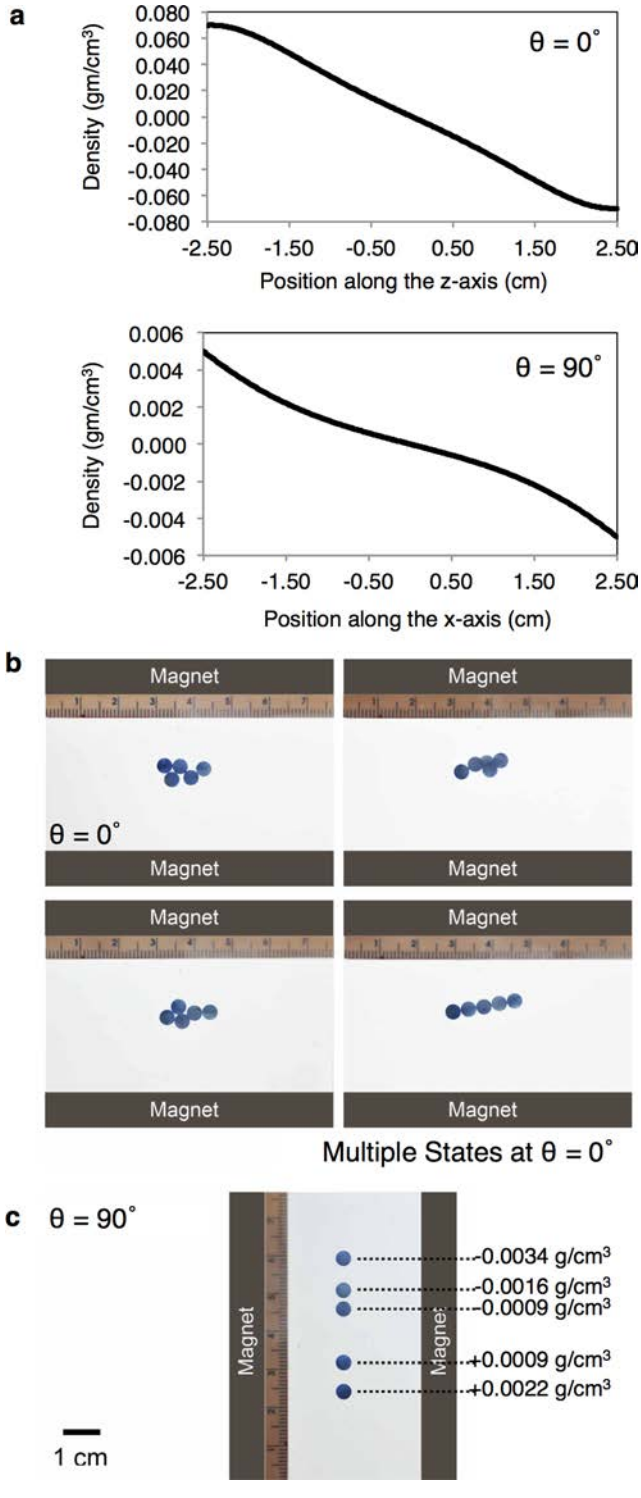

Figure 4. Tilting MagLev allows the differences in densities among objects of the same material (Nylon) to be determined. (a) Plot of comparing the sensitivity along the x- and z-axes. (b) Image of levitated beads in the standard configuration (θ = 0°) through various phases of agitation. (c) Beads in the rotated configuration (θ = 90°). We dyed the beads blue (disperse blue dye) for better visualization, although undyed beads demonstrated the same effect (as shown in the SI).

DOI: 10.1021/acs.analchem.5b03918
Anal. Chem. 2016, 88, 2666−2674

improved the resolution to $\Delta\rho_{min} = 10^{-4}$ g/cm^3, while reducing the accommodated range of densities to a range of 0.0150 g/cm^3). Using the measured positions of the five beads and the magnetic profiles calculated with COMSOL, we estimated the densities of all the beads to lie within a range of $\Delta\rho = 0.0056$ g/cm^3. These results indicate that the five beads used in this experiment all differed in density, and therefore, composition, even though they were all supplied in the same batch, by the same manufacturer.

To characterize PMMA spheres, we increased the sensitivity even further by using an elongated, 3 × 1 MagLev configuration (NdFeB magnets; N42; $L \times W \times H$ = 6 in. × 2 in. × 1 in.). Figure 5a shows the experimental setup (described in Figure S3) in which we levitated several PMMA beads ($^1/_8$ in. diameter) in a solution of 1.886 M $MnCl_2$. Figure 5b shows the calculated sensitivity along the x-axes of this configuration for three different distances (d = 3.2, 14.5, and 18.9 cm). Figure 5c shows how, in the initial state (d = 3.2 cm), the sensitivity was too low and the spheres remained in hard contact. Figure 5c–f show how as we moved the magnets apart, the sensitivity increased and the difference in density became easier to resolve.

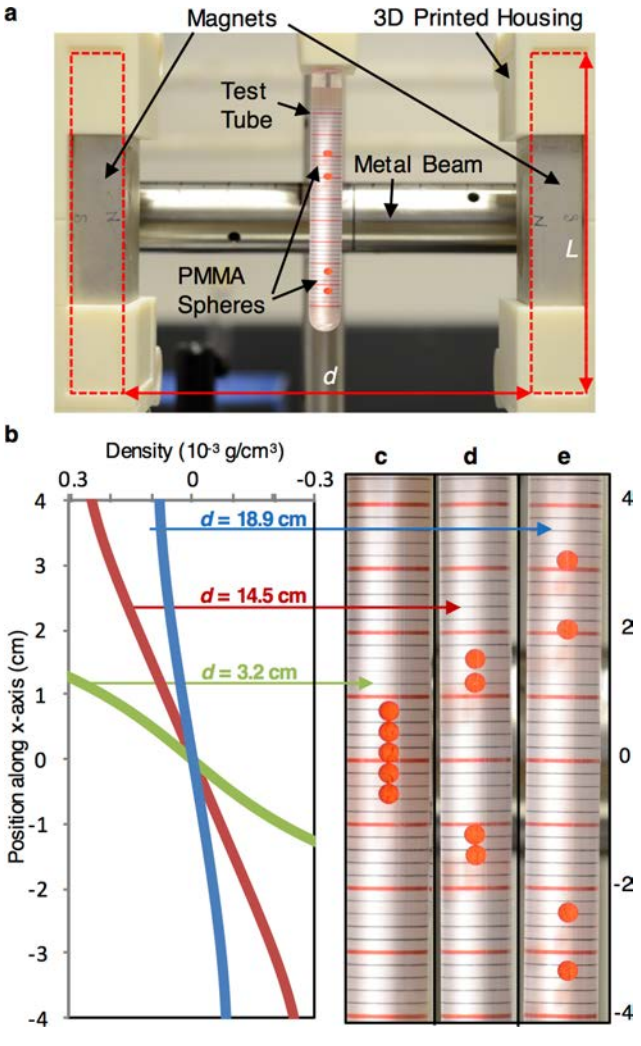

Figure 5. (a) Experimental setup showing PMMA spheres levitated in a test tube in the rotated configuration (θ = 90°) of the 3 × 1 geometry. (b) Calculated plot of the position vs density for the three configurations we tested (labeled arrows). PMMA spheres levitated when d = 3.2 cm (c), d = 14.5 cm (d), and d = 18.9 cm (e). Red markings along the test tube correspond to 1 cm spacing. In (d) and (e) the top bead drifted outside the range of the MagLev. Images shown in (c)–(e) are close-ups of the test tube shown in (a) for different values of d. In particular, the image in (d) is a cropped version of the image shown in (a).

The highest sensitivity geometry that we tested (d = 18.9 cm) increased the sensitivity by ∼80× ($S_x = 5.2 \times 10^5$ mm/(g/cm^3)), within the linear region of ∼±3 cm), relative to the rotated 2 × 1 configuration, provided a minimum resolution $\Delta\rho_{min} = 2 \times 10^{-6}$ g/cm^3 (100× better than the best resolution reported previously),[29] and provided a range of $\Delta\rho = 1.6 \times 10^{-4}$ g/cm^3. Using the measured heights of levitation and the magnetic profiles calculated with COMSOL, we estimated the smallest difference in measured density to be $\Delta\rho = 1.4 \times 10^{-5}$ g/cm^3, which occurred between the bottom two beads shown in Figure 5e. These results indicate that elongating the magnets can improve the resolution beyond what has been reported previously using MagLev, and therefore, to differentiate between "identical" PMMA spheres. We include more details, including the procedure for calibration, in the Supporting Information.

In our final application, we examined the distribution in density of small particles (e.g., millimeter-sized) by rotating MagLev. Figure 6a shows drug capsules that contained small (∼millimeter-sized) drug spheres. We used the 2 × 1 configuration because it provided the right balance between sensitivity and range to characterize the distribution of densities of the drug spheres. We determined empirically that adding $ZnCl_2$ to a paramagnetic solution of $GdCl_3$ enabled us to tune the central density of the solution and the range independently. A solution of 2.25 M $ZnCl_2$ in 0.50 M $GdCl_3$ centered the density of the solution to 1.3284 g/cm^3, the apparent mean density of the spheres and allowed all spheres to remain within the 0.07-g/cm^3 range of the standard configuration (S_z = 590 mm/(g/cm^3); $\Delta\rho_{min} = 2 \times 10^{-3}$ g/cm^3). Figure 6b shows the distribution of the spheres in the MagLev in this configuration (θ = 0°). Due to the hard contact (excluded volume) of the spheres, this configuration was not sensitive enough to analyze the distribution of densities properly. Figure 6c shows how rotating the device to θ = 90° enabled us to increase sensitivity by $S_z/S_x \sim 10$ ($S_x = 6.3 \times 10^{-4}$ mm/(g/cm^3)) ; $\Delta\rho_{min} = 2 \times 10^{-4}$ g/cm^3) relative to the standard[26] configuration and "zoom in" on a narrow range of densities (range = 0.0078 g/cm^3) close to that of the solution. These results indicate that rotated MagLev can be used for quality control of drug spheres.

■ CONCLUSIONS

This work builds on our previous work investigating tilting[44] for increasing range and applying MagLev to problems in quality control,[35] where we demonstrated that variations in density could be characterized by the orientation of a levitated component. Here we show that controlling the orientation and aspect ratio of the MagLev device itself yields another practical means of characterizing the range of quality of otherwise indistinguishable materials, simply and rapidly. "Rotated MagLev" uses the relatively weak gradients along the x- and y-axes of a MagLev device to increase sensitivity to small differences in density. We envision that the most practical implementation of MagLev for high-sensitivity measurements would be with a standalone device (similar to the one shown in Figures 5 and S3) that fixes the magnets in the rotated configuration (θ = 90°). In this configuration, samples remain collinear and the sensitivity is semilinear. Gradual tilting could

DOI: 10.1021/acs.analchem.5b03918
Anal. Chem. 2016, 88, 2666–2674

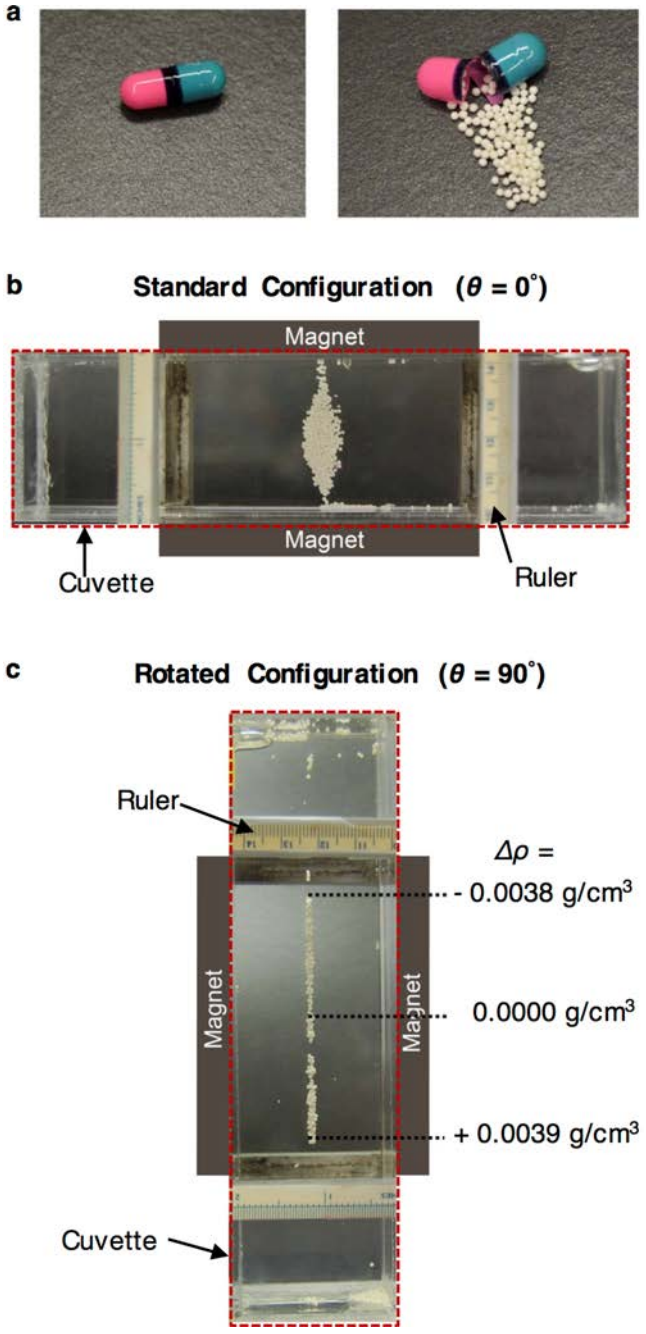

Figure 6. Examining density distribution of drug spheres. (a) Images showing drug capsules containing white drug spheres. (b) Drug spheres levitated magnetically in the standard configuration ($\theta = 0°$) of the 2 × 1 geometry. (c) Drug spheres levitated magnetically in the high sensitivity configuration ($\theta = 90°$). Measuring along the axis of high sensitivity enables the distribution of density to be examined with greater detail. The labeled densities refer to the relative density $\Delta\rho = \rho_s - \rho_m$ between the drug spheres and medium. The part of the cuvette that extends beyond the magnets enables a sharp discrimination between drug spheres that are in range and those that are out of range of the rotated configuration.

enable a user to tune sensitivity continuously, but this approach may not be practical due to the nonlinear distributions of densities at intermediate angles. As we show in this paper, a more practical approach is to first fix the device in the rotated configuration, and then tune either the distance between the magnets or the length of the magnets along the axis of measurement.

The improved resolution of rotated MagLev (shown here down to $\Delta\rho_{min} = 2 \times 10^{-6}$ g/cm^3) is sufficient to quantify the minute differences between indistinguishable samples of manufactured materials and can provide up to 100× improvement in resolution over previously reported results,[29] which used the standard MagLev configuration (faces of the magnets configured perpendicular to the gravitational field; $\theta = 0$). Another advantage of the rotated configuration is that the open side of the container remains unobscured by a magnet (as it is in the standard configuration); this geometry enables simple addition or removal of materials to and from the container, or adjustment of the properties of the medium (e.g., by adding more salt to tune the susceptibility and/or density of the medium), without disturbing the container, and therefore, suggests a path that might allow incorporation of this technique into a high-throughput, industrial setting.

In principle, the sensitivity of rotated MagLev can be increased arbitrarily by further reducing the magnetic gradient along a chosen axis through either elongating the magnets along that axis, or increasing the distance between the magnets. There are, however, three primary limitations of this procedure. (i) As the sensitivity is increased, the range of densities that can be measured is reduced, and it may become difficult to match the density of the solution and object so that they remain in range of the MagLev. (ii) Very-high-sensitivity configurations also tend to have a nonlinear field gradient. This characteristic does not prevent accurate measurements of density, but makes the process more complicated than in the linear case, where the distance between objects is directly proportional to their difference in density. (iii) Ascertaining specific heights of two objects with very similar densities in a high-sensitivity configuration is difficult because thermal variations cause shifts in the density of the paramagnetic solution on the same order as the density difference between objects. To convert the improved resolution that we achieve here into increased accuracy and precision of measurement, it would be necessary to (i) use additional equipment for thermal stabilization and (ii) perform rigorous calibration using standards better than those that are commercially available—for example, by the method we have recently reported[47] that uses aqueous multiphase systems of polymers to fractionate and improve the distribution of densities of microsphere standards from 0.006 to 0.0003 g/cm^3.

By increasing the sensitivity of MagLev, we have broadened the range of possible applications where this method can be employed. The simplicity of MagLev combined with the potential to use it in a continuous-flow process[48] and the ability to separate cells[39] (i) provides a valuable alternative to other methods of measuring density that are too inaccurate, cumbersome, or complicated for general applications, (ii) should enable the ability to monitor small changes in density in cells, and (iii) suggests the possibility of incorporating MagLev in an industrial process where continuous measurement or separation is needed.

■ ASSOCIATED CONTENT

Supporting Information

The Supporting Information is available free of charge on the ACS Publications website at DOI: 10.1021/acs.analchem.5b03918.

DOI: 10.1021/acs.analchem.5b03918
Anal. Chem. 2016, 88, 2666−2674

Figures S-1 to S-4, Table S-1, and the following sections: (i) supporting methods, results, and discussion; (ii) calibration of magnets for simulating the magnetic field; (iii) analytical calculation of isoangular and isodensity curves for rotating MagLev; (iv) calculation of magnetic susceptibility of the medium and sample; (v) construction of rotated maglev device with a 3 × 1 aspect ratio; (vi) safety considerations for handling NdFeB magnets; (vii) calibration of the high-sensitivity 3 × 1 configuration; (viii) analysis and discussion regarding the use of the 3 × 1 configuration to characterize PMMA spheres; (ix) detailed description of levitation of drug spheres; (x) supporting references (PDF)

AUTHOR INFORMATION

Corresponding Authors

*alex.nemiroski@gmail.com.

*gwhitesides@gmwgroup.harvard.edu.

Author Contributions

The manuscript was written through contributions of all authors. All authors have given approval to the final version of the manuscript.

Notes

The authors declare no competing financial interest.

ACKNOWLEDGMENTS

Preliminary work was funded by the Bill and Melinda Gates Foundation under award 51308, as well as salary support for A.N. and S.S. A.A.K. acknowledges support from the Office of Naval Research through the NDSEG fellowship program. H-D.Y. acknowledges the Agency for Science, Technology and Research (A*STAR) International Fellowship from the Singapore Government. D.V.H acknowledges salary support from Transient Electronics, Inc.

REFERENCES

(1) Gupta, S. V. *Practical Density Measurement and Hydrometry*; Taylor and Francis, 2002.

(2) Gillum, D. R. *Industrial Pressure, Level, and Density Measurement*; International Society of Automation, 2009.

(3) Irudayaraj, J.; Reh, C. *Nondestructive Testing of Food Quality*; Wiley, 2008 10.1002/9780470388310.

(4) Lachenmeier, D.; Walch, S.; Kessler, W. *Eur. Food Res. Technol.* **2006**, *223*, 261−266.

(5) Pratas, M. J.; Freitas, S. V. D.; Oliveira, M. B.; Monteiro, S. C.; Lima, Á. S.; Coutinho, J. A. P. *Energy Fuels* **2011**, *25*, 2333−2340.

(6) Sparks, D.; Smith, R.; Straayer, M.; Cripe, J.; Schneider, R.; Chimbayo, A.; Anasari, S.; Najafi, N. *Lab Chip* **2003**, *3*, 19−21.

(7) Ligas, J. R.; Moslehi, F.; Epstein, M. A. F. *Ann. Biomed. Eng.* **1993**, *21*, 361−365.

(8) Kumar, A. A.; Patton, M. R.; Hennek, J. W.; Lee, S. Y. R.; D'Alesio-Spina, G.; Yang, X.; Kanter, J.; Shevkoplyas, S. S.; Brugnara, C.; Whitesides, G. M. *Proc. Natl. Acad. Sci. U. S. A.* **2014**, *111*, 14864−14869.

(9) Kumar, A. A.; Chunda-Liyoka, C.; Hennek, J. W.; Mantina, H.; Lee, S. Y. R.; Patton, M. R.; Sambo, P.; Sinyangwe, S.; Kankasa, C.; Chintu, C.; Brugnara, C.; Stossel, T. P.; Whitesides, G. M. *PLoS One* **2014**, *9*, e114540.

(10) Chou, I.; Blank, J.; Goncharov, A.; Mao, H.; Hemley, R. *Science* **1998**, *281*, 809−812.

(11) Ochs, F.A., III; Lange, R. *Science* **1999**, *283*, 1314−1317.

(12) Valencia, J. L.; González-Salgado, D.; Troncoso, J.; Peleteiro, J.; Carballo, E.; Romaní, L. *J. Chem. Eng. Data* **2009**, *54*, 904−915.

(13) Scharlin, P.; Steinby, K.; Domańska, U. *J. Chem. Thermodyn.* **2002**, *34*, 927−957.

(14) Banipal, T. S.; Singh, G.; Lark, B. S. *J. Solution Chem.* **2001**, *30*, 657−670.

(15) Makhatadze, G. I.; Medvedkin, V. N.; Privalov, P. L. *Biopolymers* **1990**, *30*, 1001−1010.

(16) Iqbal, M. J.; Chaudhry, M. A. *J. Chem. Thermodyn.* **2009**, *41*, 221−226.

(17) Jóźwiak, M.; Tyczyńska, M. *J. Chem. Eng. Data* **2012**, *57*, 2067−2075.

(18) Patil, P.; Ejaz, S.; Atilhan, M.; Cristancho, D.; Holste, J. C.; Hall, K. R. *J. Chem. Thermodyn.* **2007**, *39*, 1157−1163.

(19) Segovia, J. J.; Fandiño, O.; López, E. R.; Lugo, L.; Carmen Martín, M.; Fernández, J. *J. Chem. Thermodyn.* **2009**, *41*, 632−638.

(20) Schaedler, T. A.; Jacobsen, A. J.; Torrents, A.; Sorensen, A. E.; Lian, J.; Greer, J. R.; Valdevit, L.; Carter, W. B. *Science* **2011**, *334*, 962−965.

(21) Fan, H.; Hartshorn, C.; Buchheit, T.; Tallant, D.; Assink, R.; Simpson, R.; Kissel, D. J.; Lacks, D. J.; Torquato, S.; Brinker, C. J. *Nat. Mater.* **2007**, *6*, 418−423.

(22) Akasaka, K.; Latif, A. R. A.; Nakamura, A.; Matsuo, K.; Tachibana, H.; Gekko, K. *Biochemistry* **2007**, *46*, 10444−10450.

(23) Kikuchi, T.; Wang, B. S.; Pikal, M. J. *J. Pharm. Sci.* **2011**, *100*, 2945−2951.

(24) Li, Y.; Guo, Q.; Kalb, J. A.; Thompson, C. V. *Science* **2008**, *322*, 1816−1819.

(25) Zhu, Y.; Demilie, P.; Davoine, P.; Delplancke-Ogletree, M.-P. *J. Cryst. Growth* **2004**, *263*, 459−465.

(26) Zelenyuk, A.; Cai, Y.; Chieffo, L.; Imre, D. *Aerosol Sci. Technol.* **2005**, *39*, 972−986.

(27) Eren, H. Chapter 21. In *The Measurement, Instrumentation and Sensors Handbook*; CRC Press, 1999.

(28) Dreisbach, F.; Lösch, H. W. *J. Therm. Anal. Calorim.* **2000**, *62*, 515−521.

(29) Mirica, K. A.; Shevkoplyas, S. S.; Phillips, S. T.; Gupta, M.; Whitesides, G. M. *J. Am. Chem. Soc.* **2009**, *131*, 10049−10058.

(30) Mirica, K. A.; Phillips, S. T.; Shevkoplyas, S. S.; Whitesides, G. M. *J. Am. Chem. Soc.* **2008**, *130*, 17678−17680.

(31) Shapiro, N. D.; Mirica, K. A.; Soh, S.; Phillips, S. T.; Taran, O.; Mace, C. R.; Shevkoplyas, S. S.; Whitesides, G. M. *J. Am. Chem. Soc.* **2012**, *134*, 5637−5646.

(32) Mirica, K. A.; Phillips, S. T.; Mace, C. R.; Whitesides, G. M. *J. Agric. Food Chem.* **2010**, *58*, 6565−6569.

(33) Lockett, M. R.; Mirica, K. A.; Mace, C. R.; Blackledge, R. D.; Whitesides, G. M. *J. Forensic Sci.* **2013**, *58*, 40−45.

(34) Subramaniam, A. B.; Yang, D.; Yu, H.-D.; Nemiroski, A.; Tricard, S.; Ellerbee, A. K.; Soh, S.; Whitesides, G. M. *Proc. Natl. Acad. Sci. U. S. A.* **2014**, *111*, 12980−12985.

(35) Hennek, J. W.; Nemiroski, A.; Subramaniam, A. B.; Bwambok, D. K.; Yang, D.; Harburg, D. V.; Tricard, S.; Ellerbee, A. K.; Whitesides, G. M. *Adv. Mater.* **2015**, *27*, 1587−1592.

(36) Mirica, K. A.; Ilievski, F.; Ellerbee, A. K.; Shevkoplyas, S. S.; Whitesides, G. M. *Adv. Mater.* **2011**, *23*, 4134−4140.

(37) Tasoglu, S.; Kavaz, D.; Gurkan, U. A.; Guven, S.; Chen, P.; Zheng, R.; Demirci, U. *Adv. Mater.* **2013**, *25*, 1137−43−1081.

(38) Tasoglu, S.; Yu, C. H.; Gungordu, H. I.; Guven, S.; Vural, T.; Demirci, U. *Nat. Commun.* **2014**, *5*, 4702.

(39) Durmus, N. G.; Tekin, H. C.; Guven, S.; Sridhar, K.; Arslan Yildiz, A.; Calibasi, G.; Ghiran, I.; Davis, R. W.; Steinmetz, L. M.; Demirci, U. *Proc. Natl. Acad. Sci. U. S. A.* **2015**, *112*, E3661−E3668.

(40) Knowlton, S.; Yu, C. H.; Jain, N.; Ghiran, I. C.; Tasoglu, S. *PLOS One* **2015**, *10*, e0134400.

(41) Laesecke, A.; Fortin, T. J.; Splett, J. D. *Energy Fuels* **2012**, *26*, 1844−1861.

(42) Richardson, M. G.; Wissler, R. N. *Anesthesiology* **1996**, *85*, 326−330.

(43) Feistel, R.; Weinreben, S.; Wolf, H.; Seitz, S.; Spitzer, P.; Adel, B.; Nausch, G.; Schneider, B.; Wright, D. G. *Ocean Sci. Discuss.* **2009**, *6*, 1757−1817.

DOI: 10.1021/acs.analchem.5b03918
Anal. Chem. 2016, 88, 2666−2674

(44) Nemiroski, A.; Soh, S.; Yu, H.-D.; Kwok, S. W.; Whitesides, G. M. *J. Am. Chem. Soc.* **2016**, *138*, 1252−1257.
(45) Bwambok, D. K.; Thuo, M. M.; Atkinson, M. B. J.; Mirica, K. A.; Shapiro, N. D.; Whitesides, G. M. *Anal. Chem.* **2013**, *85*, 8442−8447.
(46) Kumar, A. A.; Walz, J. A.; Gonidec, M.; Mace, C. R.; Whitesides, G. M. *Anal. Chem.* **2015**, *87*, 6158−6164.
(47) Bloxham, W. H.; Hennek, J. W.; Kumar, A. A.; Whitesides, G. M. *Anal. Chem.* **2015**, *87*, 7485−7491.
(48) Winkleman, A.; Perez-Castillejos, R.; Gudiksen, K. L; Phillips, S. T; Prentiss, M.; Whitesides, G. M *Anal. Chem.* **2007**, *79*, 6542−6550.

DOI: 10.1021/acs.analchem.5b03918
Anal. Chem. 2016, 88, 2666−2674